Synthesis of Polystyrene−Polylactide Bottlebrush Block Copolymers and Their Melt Self-Assembly into Large Domain Nanostructures

Javid Rzayev[†]

Department of Chemistry, University at Buffalo, The State University of New York, Buffalo, New York 14260-3000

Received October 13, 2008; Revised Manuscript Received January 24, 2009

ABSTRACT: High molecular weight polystyrene−polylactide (PS−PLA) bottlebrush block copolymers have been shown to self-assemble into highly ordered lamellae structures with domain spacings as large as 163 nm, as identified by ultrasmall-angle X-ray scattering. Bottlebrush block copolymers were synthesized by a combination of living radical and ring-opening polymerizations. The backbone was prepared by RAFT block copolymerization of solketal methacrylate (SM) and 2-(bromoisobutyryl)ethyl methacrylate (BIEM). Polystyrene branches were grafted by ATRP from poly(BIEM) block, and PLA branches were grafted from the poly(SM) block after the removal of ketal groups. The investigation into the self-assembly of PS−PLA bottlebrush block copolymers with varying lengths of branches and backbones revealed a number of unusual trends, which were attributed to their dynamic, three-dimensional structure. The results suggest that in phase-separated melts the bottlebrush block copolymer backbone, while extended, still possesses a certain degree of flexibility to accommodate for different interfacial areas necessary to pack into lamellae microstructures.

Introduction

Self-assembly of block copolymers into nanostructured morphologies is a versatile tool for organizing soft matter at the nanometer scale.[1] Numerous applications of block copolymers in nanotechnology have been proposed owing to the diverse array of structures that can be achieved and the ability to easily tune their physical and chemical characteristics. Thus, there is an increasing interest in block copolymers for preparing nanostructured networks, nanoporous membranes, drug delivery vehicles, nanoparticle templates, and masks for nanolithography.[2−5] Nanomaterials with large domain spacing (>100 nm) are desirable in a variety of applications, such as photonics and ultrafiltration, but they are difficult to obtain by the self-assembly of linear block copolymers. This report demonstrates the fabrication of highly ordered nanostructured materials with domain spacings larger than 100 nm by using block copolymers with bottlebrush architecture (Figure 1).

The phase behavior of an AB diblock copolymer[6] is determined by its composition f (volume fraction of one of the components) and the segregation strength parameter χN, where N is the total number of segments in the polymer chain and χ is the A−B segment−segment (Flory−Huggins) interaction parameter.[7] Upon cooling from a disordered melt (i.e., increasing χ), at a certain temperature T_{ODT} (order−disorder transition), microphase separation occurs where polymer chains organize themselves into different morphologies to minimize the contacts between A and B domains under the constraints of connectivity and overall incompressibility. Depending on composition, lamellae, cylindrical, gyroid, or spherical morphologies are produced. Typically, linear block copolymers with molecular weights in the 10−100 kg/mol range are used, which results in domain sizes of 10−40 nm. Larger domain spacings (100 nm and beyond) are very difficult to obtain due to a combination of factors.[8−10] (1) The synthesis of very high molecular weight linear block copolymers that are necessary to achieve microdomain dimensions of 100 nm and larger is very challenging. (2) High molecular weight polymers are highly entangled in the melt and therefore cannot easily self-assemble into ordered structures.

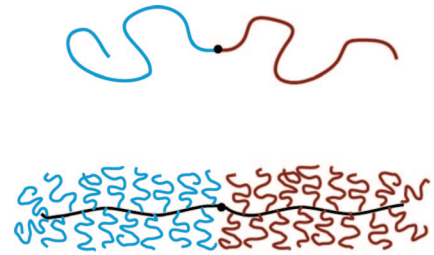

Figure 1. Linear (top) and bottlebrush (bottom) block copolymer architecture.

Bottlebrush copolymers are comblike macromolecules with highly densely grafted polymeric branches. The repulsive forces between the adjacent branches are believed to cause the backbone to stretch out and result in rigid cylindrical macromolecules (when the backbone is much longer than the branches).[11−14] Detailed investigations of bottlebrush polymer melts and nondilute solutions by scattering and rheological techniques have shown that their dynamics are governed by individual relaxation of branches, in direct analogy to the behavior of star polymers.[15−19] Bottlebrush copolymer melts are mostly unentangled, which can be attributed to their densely branched architecture and large cross-sectional area.[19] However, it has been noted that a significant increase in the backbone length can lead to intermolecular chain entanglements, albeit with low density.[18] Also, an increase in the branch length can cause strong intermolecular couplings of branches. In some cases, mesomorphic phases have been observed in concentrated bottlebrush polymer solutions,[20−22] but not in melt,[23,24] while other studies point out the decrease in persistence length (stiffness) at high concentrations.[25] Recently, Runge et al. observed nanostructure formation in a solvent-cast film of a comb diblock copolymer with a total molecular weight of 36×10^6 g/mol.[26] Runge et al. also synthesized comb−linear diblock copolymers based on polynorbornene backbone that self-assemble into well-ordered nanostructures.[27]

High molecular weight bottlebrush copolymers can be synthesized either by grafting-through[28] or grafting-from[29] methods. In the grafting-through approach, macromonomers, which are polymer chains with reactive end groups, are prepared

[†] E-mail: jrzayev@buffalo.edu.

10.1021/ma802304y CCC: $40.75

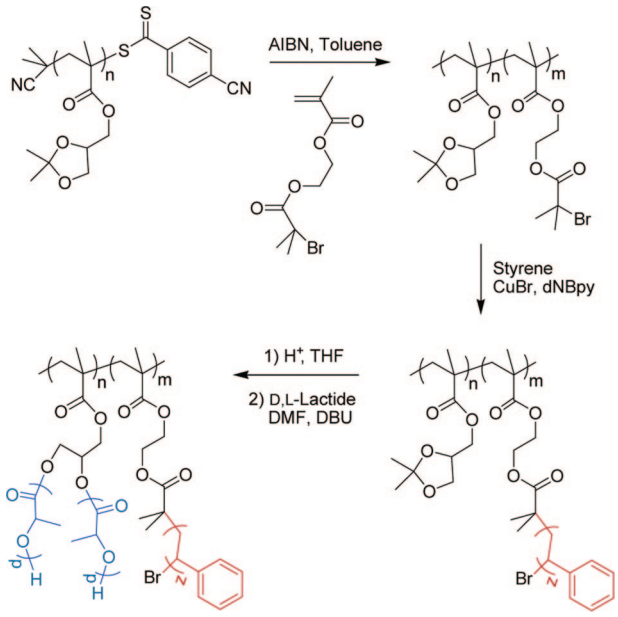

Figure 2. Synthesis of PS−PLA bottlebrush block copolymers.

first and then polymerized to provide comb architecture. In the grafting-from method, a polymer backbone with multiple initiator sites is synthesized first, and branches are then grafted from the backbone via a polymerization of suitable monomers. Comb polymers with homopolymer and block copolymer branches have been prepared by both of these methods. Recently, Lee et al. reported the synthesis of bottlebrush copolymer with a diblock backbone and their single molecule visualization by atomic force microscopy.[30]

I contend that entanglement-free dynamics of high molecular weight bottlebrush *block* copolymers will allow their self-assembly into well-ordered large domain nanostructures, in contrast to their linear analogues. In this report, I describe novel synthesis of polystyrene−polylactide (PS−PLA) bottlebrush block copolymers by a combination of living radical and ring-opening polymerization protocols and characterization of their melt self-assembly by ultrasmall-angle X-ray scattering.

Experimental Section

Materials. Azobis(isobutyronitrile) (AIBN) was recrystallized from methanol, DL-lactide was recrystallized from ethyl acetate, and DMF was dried using a commercial solvent purification system (Innovative Inc.); all other chemicals were used without further purification unless stated otherwise. Solketal methacrylate (SM),[31] 2-(bromoisobutyryl)ethyl methacrylate (BIEM),[32] and 2-cyanoisopropyl 4-cyanodithiobenzoate (CTB)[33] were synthesized according to the literature procedures.

Poly(SM). Solketal methacrylate (2 mL, 10 mmol), CTB (13 mg, 53 μmol), and AIBN (0.8 mg, 5.3 μmol) were dissolved in 1 mL of toluene and placed in a reaction tube. The mixture was degassed by three cycles of freeze−pump−thaw, sealed, and placed in an oil bath at 65 °C. After 16 h, the contents were diluted with dichloromethane and precipitated in methanol (twice). The polymer was filtered and dried in a vacuum oven overnight. Yield = 1.5 g. GPC (light scattering detector): M_n = 42.8 kg/mol, M_w/M_n = 1.05.

Poly(BIEM). 2-(Bromoisobutyryl)ethyl methacrylate (1 mL, 4.7 mmol), CTB (2.9 mg, 12 μmol), and AIBN (0.19 mg, 1.2 μmol) were dissolved in 0.5 mL of toluene in a reaction tube. The mixture was degassed by three freeze−pump−thaw cycles, sealed, and allowed to react for 16 h at 65 °C. The polymer was precipitated in methanol (twice), filtered, and dried. Yield = 0.47 g. GPC (light scattering detector): M_n = 71.0 kg/mol, M_w/M_n = 1.05.

Poly(SM-*b*-BIEM). Poly(SM) (M_n = 42 800, 0.2 g) was dissolved in a mixture of BIEM (0.43 mL, 2 mmol) and toluene (0.1 mL) in a reaction tube. The mixture was stirred at room temperature until the polymer completely dissolved. Then, AIBN (8.5×10^{-2} mg, 4.9 μmol) was added to the tube, and the mixture was degassed by three freeze−pump−thaw cycles. The polymerization was run at 65 °C for 25 h. The reaction mixture was cooled down under running water, diluted with dichloromethane, and precipitated in methanol (twice). The product was filtered and dried in a vacuum oven. Yield = 0.41 g. GPC (polystyrene standards): M_n = 35.2 kg/mol, M_w/M_n = 1.16.

Polystyrene Grafting. Styrene was bubbled with nitrogen for 20 min in a septum-capped flask to remove oxygen. Poly(SM-*b*-BIEM) initiator (50 mg, 95 μmol of bromide groups) and a stirbar were placed in a reaction tube, evacuated, and refilled with nitrogen three times. Deoxygenated styrene (1.3 mL) was then added to the reaction tube via syringe under constant nitrogen flow, and the contents were stirred for 1 h. In a separate flask with a side arm, CuBr (6.8 mg, 47 μmol), $CuBr_2$ (1.6 mg, 7.2 μmol), and 4,4′-dinonylbipyridine (45 mg, 0.11 mmol) were mixed, evacuated, and refilled with nitrogen three times. Deoxygenated styrene (2 mL) was added to the flask containing the catalyst mixture, and the contents were stirred at room temperature under nitrogen until a homogeneous brown-red catalyst solution was obtained (∼1 h). Afterward, the catalyst solution was transferred to the reaction tube via nitrogen flashed syringe, and the polymerization was carried out for 18 h at 90 °C. At the end of the reaction, the mixture was cooled down and precipitated in methanol (twice). White powdery polymer was filtered and dried in vacuum. Yield = 0.36 g. ^{1}H NMR: M_n (PS branch) = 3.2 kg/mol. GPC (polystyrene standards): M_n = 137 kg/mol, M_w/M_n = 1.18.

Hydrolysis of Poly(SM). Polystyrene grafted poly(SM-*b*-BIEM) (0.15 g) was dissolved in 4 mL of THF. Hydrochloric acid (1 M, 0.1 mL) was added dropwise to the solution, and the mixture was stirred at room temperature for 18 h. The polymer was precipitated in methanol (twice), filtered, and dried.

Polylactide Grafting. Deprotected poly(SM-*b*-(BIEM-*g*-St)) (50 mg) and DL-lactide (120 mg) were placed in a flame-dried flask, evacuated, and refilled with nitrogen three times. Dry DMF (1 mL) was then added under nitrogen, and the mixture was stirred until all polymer dissolved. DBU was then injected into the flask, and the reaction was carried out at room temperature for 2 h. The polymerization was quenched by adding benzoic acid (8 mg), the mixture was diluted with dichloromethane, and the polymer was precipitated in methanol (twice). Yield = 120 mg. ^{1}H NMR: M_n (PLA branch) = 2.9 kg/mol, grafting density = 86%.

PS Branch Cleavage. Bottlebrush block copolymers (20 mg) were dissolved in 1 mL of THF, and 10 drops of 5 M KOH (in methanol) were added. The mixture was sealed and heated at 60 °C for 2 days. After the solution was cooled down, it was concentrated to contain about 0.2 mL of solvent, and the polymers were precipitated in methanol, centrifuged, and dried.

Measurements. GPC analysis was performed by using Viscotek's GPCMax and TDA302 Tetradetector Array system equipped with two PolyPore columns (Polymer Laboratories, Varian Inc.). The detector unit contained a refractive index, UV, viscosity, low (7°), and right angle light scattering modules. Measurements were carried out in THF as a mobile phase at 30 °C. The system was calibrated with 10 polystyrene standards from 1.2×10^6 to 500 g/mol. Refractive index increments (dn/dc) for poly(SM) and poly(BIEM) were measured to be 0.067 and 0.074 mL/g in THF (T = 30 °C, λ = 630 nm), respectively, and were used to determine absolute molecular weights of the homopolymers. NMR measurements were performed on a Varian Inova-500 (500 MHz) spectrometer by using $CDCl_3$ or d_6-DMSO as a solvent. Differential scanning calorimetry (DSC) analysis was conducted on a TA Instruments Q200 system with an RCS-90 cooling device. Glass transition temperatures were measured on the second heating scan at a rate of 10 °C/min. Small-angle X-ray scattering studies were carried out by using an in-house Bruker Nanostar system with a 2D area detector. Ultrasmall-angle X-ray scattering (USAXS) measurements were performed using an instrument located at the Advanced Photon Source beamline 32.[34] The USAXS data were

Table 1. Synthesis of Poly(SM-*b*-BIEM) Block Copolymers by RAFT Polymerization[a]

polymer	initiator	monomer	[M]:[I]	time (h)	M_n (kg/mol)[b]	M_w/M_n[b]	N_{SM}/N_{BIEM}[c]
PSM	CTB	SM	200:1	16	18.9 (42.8)	1.15 (1.05)	
PBIEM	CTB	BIEM	400:1	16	24.0 (71.0)	1.17 (1.05)	
SB-1	PSM	BIEM	420:1	25	53.0	1.23	2:1
SB-2	PSM	BIEM	420:1	18	35.2	1.16	1:1
SB-3	PSM	BIEM	420:1	13	27.9	1.14	1:2

[a] $T = 65$ °C; AIBN was used as a free-radical generator. [b] Measured by GPC with polystyrene calibration. The numbers in parentheses were obtained from GPC with a light scattering detector. [c] The ratio between the number of repeat units in the two blocks as calculated from NMR data.

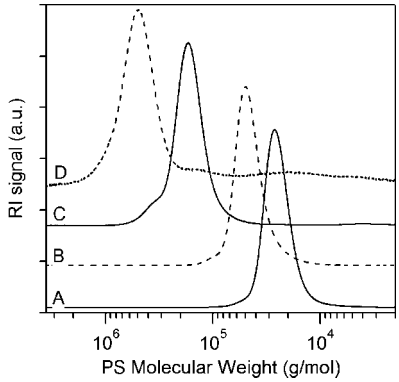

Figure 3. GPC traces of (A) poly(SM), (B) poly(SM-*b*-BIEM), (C) poly(SM-*b*-(BIEM-*g*-St)), and (D) PS−PLA bottlebrush block copolymer.

collected in the scattering vector (q) range 0.0001−1 Å^{-1}, reduced using Indra data reduction package and analyzed using Irena data analysis package. Scanning electron microscopy (SEM) images were obtained by a Hitachi SU-70 using secondary electron detector at an accelerating voltage of 2.0 kV. Prior to SEM analysis, fractured polymer samples were stained with RuO_4 vapor for 6 min and coated with a 1−2 nm carbon layer.

Results and Discussion

Polymer Synthesis. Bottlebrush block copolymers were prepared by a grafting-from method involving reversible addition−fragmentation chain-transfer (RAFT) polymerization,[35] atom-transfer radical polymerization (ATRP),[29] and ring-opening polymerization. The general synthetic strategy is outlined in Figure 2. The backbone was prepared by RAFT block copolymerization of solketal methacrylate (SM) and 2-(bromoisobutyryl)ethyl methacrylate (BIEM). Polystyrene (PS) branches were grafted by ATRP from bromide initiators on the BIEM segment of the backbone. Subsequently, ketal groups of poly(SM) were hydrolyzed to provide two hydroxyl groups per repeat unit, which were used to initiate polymerization of DL-lactide (LA).

Synthesis of the Backbone. Diblock copolymer backbone was prepared by the polymerization of SM as a precursor for pendant hydroxyl groups and direct polymerization of BIEM to install pendant bromide initiators. Other researchers have often used 2-hydroxyethyl methacrylate (HEMA) or its derivatives, such as trimethylsilyl-HEMA, to prepare bottlebrush copolymer backbones.[36,37] The choice of solketal methacrylate in this work stems from the fact that it does not possess problems associated with HEMA (dimethacrylate impurities) and HEMA-TMS (difficult polymer isolation and purification) and at the same time can be easily polymerized, characterized, and deprotected (vide infra). The direct RAFT polymerization of BIEM provided poly-ATRP initiators without the need for postpolymerization modifications.

RAFT polymerization was performed with 2-cyanoisopropyl 4-cyanodithiobenzoate (CTB) as a chain transfer agent. This particular chain transfer agent has been reported to provide superb control over the polymerization of methyl methacrylate, leading to polymers with polydispersities lower than 1.1,[33] and was therefore chosen for this work. Indeed, CTB-mediated polymerization of both SM and BIEM provided polymers with controlled molecular weights and narrow molecular weight distributions (Table 1). Block copolymers were prepared by using poly(SM) as a macrochain transfer agent for the polymerization of BIEM. The GPC analysis and the obtained low polydispersities indicated complete reinitiation and a good control over the polymerization process (Figure 3, traces A and B). A series of block copolymers were prepared with varied ratios between the two blocks, as shown in Table 1.

Polystyrene Grafting. Pendant bromide groups of the poly(BIEM) block were used to initiate polymerization of styrene by ATRP. Styrene is notorious for having a tendency to undergo termination by recombination, which can be detrimental in the case of multifunctional initiators, even in very limited amounts. To maintain very low radical concentration throughout the polymerization, Cu(I)Br with 15% $Cu(II)Br_2$ was used as a catalyst mixture.[36] The reactions were allowed to proceed up to 20% conversion in order to prevent cross-linking. At higher conversions, a significant coupling peak and cross-linking could be observed. Under optimized conditions, polystyrene grafted polymers were prepared with narrow molecular weight distributions (Table 2). Molecular weights of PS branches were calculated by NMR end-group analysis and by GPC analysis after cleaving them from the backbone. The obtained values agreed very well with those based on monomer conversions under the assumption of complete initiation. Furthermore, the area under NMR signal arising from the C*H*−Br end group of PS branches (4.4−4.6 ppm) was compared to that of solketal groups of poly(SM) (4.3 ppm) (Figure 4). The obtained ratios matched the values from the original poly(SM-*b*-BIEM), which confirmed that almost every repeat unit of poly(BIEM) contained one polystyrene side chain, and thus near-quantitative initiation (>90%) was achieved.

Polylactide Grafting. Solketal groups of PS grafted poly(SM-*b*-BIEM) brush polymers were hydrolyzed in acidic THF at room temperature. Complete deprotection was achieved in 16 h, which was confirmed by the disappearance of solketal peaks in NMR. Upon hydrolysis, the final polymer was still soluble in THF and DMF but became insoluble in chlorinated solvents. Polylactide (PLA) grafting was achieved by DBU catalyzed ring-opening polymerization[38] in dry DMF at room temperature. The reaction rate was noticeably slower than that observed for small alcohol initiators. Polymer conversions varied between 50 and 70% for a 2 h reaction time. Molecular weights of the polylactide branches were calculated by NMR end-group analysis (Table 3). At the same time, the area under the NMR signal originating from PLA end groups (4.3−4.6 ppm, see Figure 4) was compared to the PS peak to calculate the number of PLA branches per molecule. The results indicated that 70−90% of pendant hydroxyl groups initiated the polymerization of lactide. These structures, therefore, represent the most densely branched bottlebrush macromolecules reported, with an average of 1.5−1.8 branches for every two-carbon repeat unit. It must be noted that the use of relatively high lactide concentrations (0.8−1.0 mol/L) was necessary to achieve the observed high grafting densities. When reaction was conducted

Table 2. Polystyrene Grafting from Poly(SM-*b*-BIEM) by ATRP[a]

						PS branch		
polymer	initiator	time (h)	yield (%)	$M_{n,GPC}$[b] (kg/mol)	M_w/M_n[b]	$M_{n,NMR}$[c]	$M_{n,GPC}$[d]	M_w/M_n[d]
PS-1	SB-3	18	11	289	1.21	3.2	3.1	1.11
PS-2	SB-2	18	10	137	1.18	3.2	2.7	1.09
PS-3	SB-2	29	20	220	1.25	5.7	5.5	1.12
PS-4	SB-1	18	15	81.8	1.17	3.5	3.3	1.10

[a] $T = 90$ °C; [−Br]:[CuBr]:[$CuBr_2$]:[ligand] = 300:1:0.5:0.075:1.15. [b] Measured by GPC relative to polystyrene standards. [c] Calculated by NMR end-group analysis. [d] Measured by GPC after cleavage of PS branches.

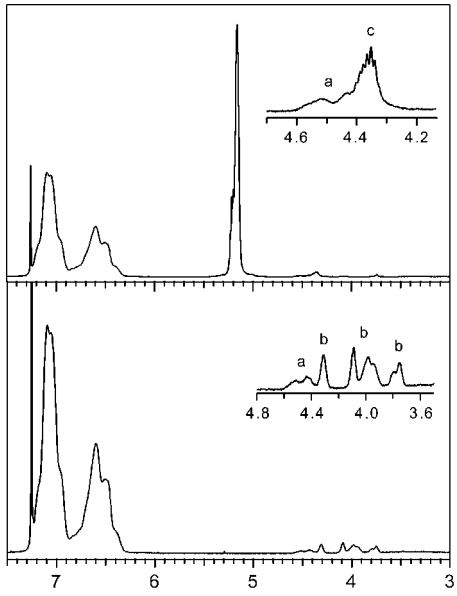

Figure 4. ^{1}H NMR spectra of poly(SM-*b*-(BIEM-*g*-St)) (bottom) and PS−PLA bottlebrush copolymers (top). The insets show peaks corresponding to (a) −C*H*Br end groups of PS branches, (b) solketal groups of poly(SM) block, and (c) −C*H*(CH_3)OH end group of PLA branches.

under more dilute conditions ([LA] = 0.35 mol/L), a significantly lower initiating efficiency of 65% was obtained (sample SL-2 in Table 3).

Characterization of the prepared PS−PLA bottlebrush copolymers by GPC proved to be challenging. While all samples exhibited a single monomodal peak that clearly shifted toward lower elution volumes (see Figure 3D), they also had long tails stretching toward the higher elution volume (smaller size) region. The light scattering signal of the tail had a similar intensity to that of the main peak (relative to the RI signal), which suggested that the tail signal was originating from the macromolecules with similar size to those eluting in the main peak and not small molecular weight chains. Similar anomalous elution behavior was observed for other high molecular weight branched polymers and was attributed to non-size-exclusion separation mechanisms.[39] The presence of the tail and possible anomalous elution behavior made it very difficult to get a reliable estimate of molecular weight distributions for the final polymers. Polydispersity indexes calculated for main peaks relative to PS standards were around 1.3−1.4, while those calculated using light scattering detector (including the tail) were lower than 1.1.

Polymer Self-Assembly. The DSC analysis of the bottlebrush block copolymers showed two separate glass transitions at 54 and 104 °C corresponding to PLA and PS domains, respectively. The presence of two T_g's indicated that block copolymers were undergoing phase separation. No other thermal transitions were detected in the temperature range of 0−250 °C.

Melt phase separation of PS−PLA bottlebrush block copolymers with varying backbone and side chain lengths was investigated in order to determine the effect of structural parameters on the formed morphologies. Polymer samples were pressed into disks and annealed at 170 °C for 16 h. While powdery samples were completely white, melt-pressed polymer disks of larger molecular weight block copolymers appeared to reflect blue light, which indicated the formation of ordered morphologies with large enough periodicities to interact with visible light (Figure 5).

The polymers were then analyzed by ultrasmall-angle X-ray scattering (USAXS). All block copolymers showed strong primary scattering peaks, confirming phase separation. Most of the samples also exhibited multiple higher order reflections, in some cases up to eight peaks, consistent with the formation of morphologies with long-range order. Figure 6 illustrates a USAXS pattern obtained for one of the block copolymers, and Table 3 summarizes *d*-spacings and morphologies obtained for all analyzed samples. Only block copolymers with large asymmetry (SL-6 and SL-7) did not show strong higher order reflection peaks, and therefore the morphology for these samples could not be identified. All other polymers appeared to pack into remarkably ordered lamellae structures. While it is not possible to ascertain that the observed structures are under thermodynamic equilibrium, prolonged annealing did not change X-ray scattering results in any way.

Scanning electron microscopy (SEM) analysis of a fractured piece of bottlebrush copolymer SL-1 confirmed the presence of a highly ordered lamellae morphology (Figure 7). Lamellae thickness obtained from SEM was in close agreement with that obtained from USAXS analysis.

Molecular Architecture. High molecular weight bottlebrush copolymers appeared to self-assemble into highly ordered morphologies upon annealing and without the need for additional processing. Such a behavior was attributed to the unentangled nature of bottlebrush copolymer melts. The polymers investigated here contained branches that were smaller than critical entanglement molecular weights (14 and 4 kg/mol for PS[40] and PLA,[41] respectively) and therefore should be mostly free of entanglements. The only morphology observed was lamellae, which is consistent with the packing of rigid macromolecules. When large asymmetry was introduced into the block copolymer structure, by varying either side chain lengths or backbone lengths of the two blocks, the order of the formed microstructures deteriorated, as indicated by the absence of higher order reflection peaks in USAXS. Such asymmetric molecules cannot easily form lamellae structures but at the same time are not flexible enough to pack into morphologies with curved interfaces.

The effect of macromolecular architecture of the bottlebrush copolymers on their packing preferences can be illustrated by comparing two block copolymers with identical chemical compositions (i.e., PS and PLA volume fractions) but different molecular architectures (SL-2 and SL-6). Block copolymer SL-2 had an asymmetric bottlebrush backbone with nearly equal PS and PLA branch lengths, while sample SL-6 consisted of a symmetric backbone with different PS and PLA branch lengths. As a result of different macromolecular architecture, the two block copolymers exhibited dissimilar self-assembly tendencies

Table 3. Structural Characteristics of the Synthesized PS−PLA Bottlebrush Block Copolymers

	N backbone		M_n branch (kg/mol)[a]						
block copolymer	PS	PLA	PS	PLA	g_{PLA}[b]	total M_n (g/mol)[c]	f_{PLA}[d]	*d*-spacing (nm)[e]	morph[f]
SL-1	420	210	3.2	2.6	1.8	2.4×10^6	0.37	153	L
SL-2	420	210	3.2	2.6	1.3	2.0×10^6	0.29	163	L
SL-3	210	210	3.0	2.9	1.7	1.7×10^6	0.57	105	L
SL-4	210	210	3.0	1.4	1.8	1.2×10^6	0.40	100	L
SL-5	210	210	5.7	3.6	1.5	2.4×10^6	0.43	126	L
SL-6	210	210	5.7	1.7	1.7	1.8×10^6	0.28	111	
SL-7	110	210	3.5	2.8	1.8	1.5×10^6	0.69	76	

[a] Calculated from NMR data by end-group analysis. [b] Number of PLA branches per repeat unit as calculated by NMR (number of PS branches per repeat unit is equal to 1). [c] Measured by NMR knowing the molecular weight of the precursor. [d] Volume fraction of PLA calculated using known densities $\rho_{PS} = 1.04$ and $\rho_{PLA} = 1.25$ g/mL. [e] Calculated from the primary scattering peak ($d = 2\pi/q_0$). [f] Morphology as identified by USAXS analysis at 25 °C after annealing at 170 °C for 16 h.

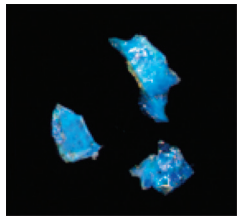

Figure 5. Optical image of fractured pieces of SL-1 after annealing.

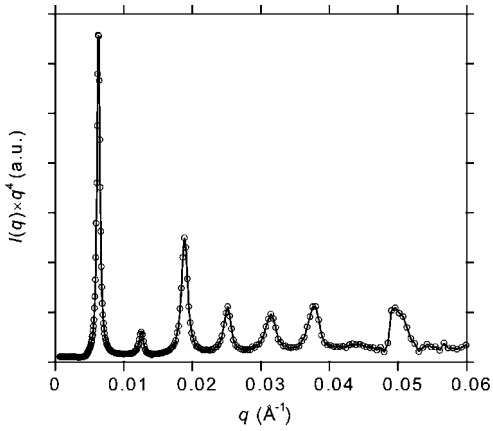

Figure 6. USAXS pattern obtained for a PS−PLA bottlebrush block copolymer (SL-4, $M_n = 1.2 \times 10^6$ g/mol, $q_0 = 0.0063$ Å^{-1}).

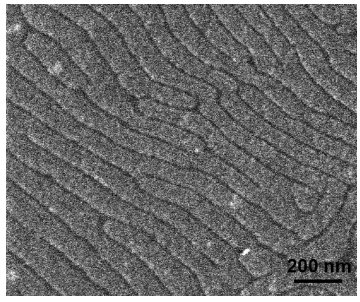

Figure 7. SEM image of a fractured piece of polymer SL-1.

(Figure 8). SL-2 packed into highly ordered lamellae microstructure, as evidenced by its USAXS profile with several diffraction peaks at multiples of q_0. Expected scattering peaks at $3q_0$ and $6q_0$ were absent due to the fact that this block polymer had a PLA volume fraction close to 1/3.[42] On the other hand, SL-6 did not exhibit well-ordered morphology. The USAXS pattern of SL-6 contained small peaks corresponding to $2q_0$ and $\sqrt{7}q_0$, which would suggest the formation of cylindrical microstructure. However, unambiguous identification of the morphology was impossible due to weak intensities of the higher order reflection peaks. It appears that side chain asymmetry

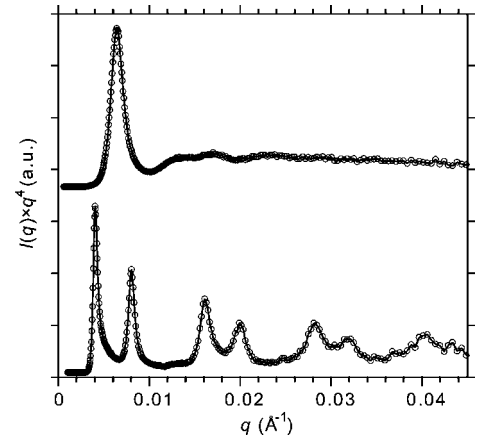

Figure 8. USAXS analysis of two PS−PLA bottlebrush copolymers with the same chemical composition but different molecular architectures: SL-2 (bottom) and SL-6 (top).

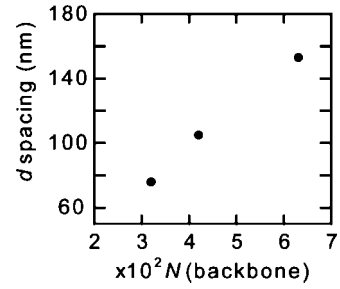

Figure 9. Dependence of *d*-spacing (USAXS) on the number of backbone repeat units for a series of PS−PLA bottlebrush copolymers with similar size branches (∼3 kg/mol).

creates packing frustrations that could not be overcome due to the rigid nature of bottlebrush macromolecules.

Backbone Effects. PS−PLA bottlebrush copolymers investigated in this work self-assembled into nanostructures with very large domain spacings, up to 163 nm, as calculated from primary scattering peaks. Since the studied block copolymers are not composed of very long backbones (maximum of 630 units), the formation of such large structures suggests a stretched-out conformation of the bottlebrush backbone. This is consistent with perpendicular orientation of bottlebrush macromolecules relative to the plane of lamellae. The dependence of the domain spacing on the bottlebrush backbone length was investigated by comparing three samples, SL-1, SL-3, SL-7, all of which have similar size branches (∼3 kg/mol) and similar branching densities but have different number of repeat units in the backbone. From the limited number of data points available (Figure 9), it appears that domain spacing increases linearly with the backbone length, therefore suggesting an extended conformation.

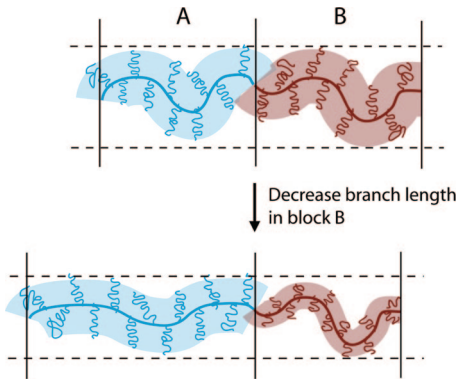

Figure 10. Illustration of backbone stretching in block A in order to match the reduced interfacial area produced as a result of decreased side chain length (or decreased grafting density) in block B.

Table 4. Lamellae Thicknesses in PS−PLA Bottlebrush Block Copolymers

polymer	d^a (nm)	$d_{PLA}{}^b$ (nm)	$d_{PS}{}^b$ (nm)
SL-1	153	57	96
SL-2	163	47	116
SL-3	105	60	45
SL-4	100	40	60
SL-5	126	54	72

[a] Domain spacing obtained from USAXS. [b] Thicknesses of PLA and PS layers calculated from domain spacings and volume fractions of the lamellae forming block copolymers.

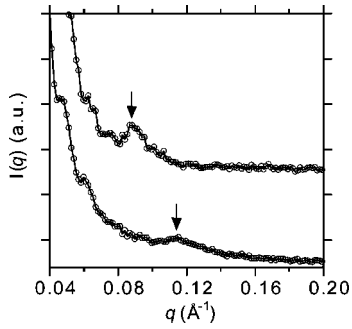

Figure 11. High q region of SAXS profiles of two PS-PLA bottlebrush block copolymers with identical backbones but different size branches: SL-4 (bottom) and SL-5 (top). Arrows indicate the positions of weak halos.

Side-Chain Effects. In a bottlebrush block copolymer, the interface between the two blocks is fixed within a polymer. To form lamellae structures, from a volume filling perspective, the cross-sectional area of PLA side of the bottlebrush has to match that of the PS side. Longer and more stretched side chains increase the cross-sectional area, while backbone stretching reduces it.

An interplay between bottlebrush polymer's cross-sectional area and its backbone stretching can be observed by comparing two block copolymers that differ only in one structural parameter. For example, polymers SL-1 and SL-2 have identical structural parameters, except for the grafting density of PLA branches. SL-2 has a grafting density of 1.3 PLA branches per repeat unit compared to 1.8 for SL-1. As a result of lower branching density, the molecular weight of SL-2 is smaller than that of SL-1 by about 400 kg/mol. However, d-spacing measured for SL-2 is larger than that of SL-1, 163 vs 153 nm, respectively. This behavior can be rationalized in terms of the interfacial areas between the two blocks (Figure 10). Knowing volume fractions and d-spacings of the lamellae structure, PS and PLA domain sizes (d_A) can be calculated separately by using the following formula: $d_A = df_A$. The calculated values for all lamellae block copolymers are provided in Table 4. The decrease in grafting density in the PLA side of the bottlebrush SL-2 leads to less steric crowding and therefore reduced stretching of the backbone and the side chains, which manifests itself in the shrinkage of the PLA domain by 10 nm compared to SL-1 (Table 4). At the same time, more relaxed PLA side chains in SL-2 result in a smaller cross-sectional area of the PLA side of the bottlebrush block copolymer. In order to compensate for that, PS side of the bottlebrush stretches out, which leads to a significant increase in PS domain size (Table 4). Overall, the lamellae domain spacing increases despite the decrease in the molecular weight of the polymer (Figure 10).

Another example of this intricate behavior can be found when comparing polymers SL-3 and SL-4 that have near identical structural parameters, except for the length of PLA branches. As a result of longer PLA branches, volume fraction of PLA is 17% higher and overall molecular weight is 500 kg/mol larger for SL-3 than for SL-4. Both polymers form lamellae microstructures; however, their domain spacings only differ by 5 nm (105 nm for SL-3 vs 100 nm for SL-4). As evident from the data in Table 4, smaller PLA branches in SL-4 result in a decreased PLA domain size (by 20 nm) compared to SL-3. However, there is a concomitant increase in PS domain size, which presumably results from backbone stretching in the PS side of the bottlebrush to match the reduced cross-sectional area of the PLA block. The two effects almost cancel out, and as a result, the domain spacing does not change much despite a significant decrease in the molecular weight of the block copolymer and PLA volume fraction.

Molecular Packing. The bottlebrush block copolymers were also analyzed by an in-house SAXS instrument with a 2D area detector. Most of the lamellae samples exhibited a diffuse halo in the high q region, which appeared as a weak peak in 1D scattering profiles (Figure 11). The position of the peak varied with the branch size. For polymer SL-4 and SL-5, scattering peaks at q equal to 0.114 and 0.885 $Å^{-1}$ were observed, accordingly. These peaks were attributed to the chemical (backbone vs branch) or density inhomogeneities arising from the molecular packing of bottlebrush copolymers in melt. Interbackbone distances corresponding to these peaks were calculated by using the following formula: $d = 1.15 \times 2\pi/q$, applicable to hexagonally packed cylinders. For SL-4 and SL-5 the interbackbone distances (or cross-sectional diameters) were calculated to be 6.3 and 8.2 nm, respectively, consistent with longer branches for SL-5 (Table 3). Such scattering due to backbone−backbone correlations have been reported previously for melt-extruded bottlebrush copolymer samples.[24] However, the authors also observed that these scattering peaks disappeared upon annealing, presumably due to the disruption of alignment achieved by extrusion. For the polymers described in this work, the peaks were stable to annealing and were attributed to the orientation of bottlebrush block copolymer chains perpendicular to the plane of lamellae during phase separation.

A number of studies on bottlebrush copolymers in dilute solutions have shown that they exist as stiff cylindrical macromolecules.[43] Recent work by Bolisetty et al. indicated that bottlebrush copolymers in concentrated solutions undergo softening, or decrease in persistence length, owing to mutual interactions.[25] The findings presented in this work suggest that in phase-separated melts the bottlebrush block copolymer backbone, while extended, still possesses a certain degree of flexibility to accommodate for different interfacial areas necessary to pack into lamellae microstructures.

Conclusions

This report demonstrates the preparation of nanostructured materials with large domain spacings (>100 nm) from block

copolymers with relatively short backbones, which can be synthesized by a combination of well-established synthetic methods. This is the first in-depth investigation into the melt self-assembly of bottlebrush block copolymers, which provided access to previously unattainable materials.

A new method for the synthesis of bottlebrush block copolymers has been developed. A diblock copolymer of solketal methacrylate and 2-(bromoisobutyryl)ethyl methacrylate served as a dual macroinitiator for lactide and styrene grafting. Poly(BIEM) block served as initiator for ATRP of styrene, while poly(SM), after hydrolysis, served as an initiator for ring-opening polymerization of lactide. Hydrolyzed poly(SM) provided two hydroxyl group per repeat unit, which resulted in very high grafting densities of PLA (up to 1.8 chains per two-carbon repeat unit). These structures represent the densest bottlebrush molecules synthesized up to date.

The prepared PS−PLA bottlebrush block copolymers phase-separated into highly ordered lamellae microstructures in melt. The facile self-assembly of such large molecular weight macromolecules (up to 2.4 million g/mol) was attributed to the low number of entanglements. Lamellae microstructures were characterized by USAXS, and their domain spacings were found to be as large as 163 nm. The size of the lamellae pitch appeared to vary linearly with the number of backbone units of a bottlebrush copolymer, suggesting a stretched out conformation. A number of unusual trends in the self-assembly of asymmetric bottlebrush macromolecules were attributed to their dynamic three-dimensional structure. Thus, a decrease in the size of the side chains in one of the blocks led to a backbone stretching in the other block in order to accommodate for a smaller cross-sectional area.

The exclusive formation of lamellae morphologies was consistent with the semirigid nature of bottlebrush macromolecules. Highly asymmetric block copolymers did not appear to assemble into ordered structures. Such molecules cannot maintain a constant cross-sectional area to form lamellae morphologies, and they are not flexible enough to pack into microstructures with curved interfaces. Currently, we are exploring blending of bottlebrush block copolymers with linear homopolymers and the use of flexible linkers between two bottlebrush blocks in an attempt to diversify the pool of attainable microstructures.

Acknowledgment. I thank the University at Buffalo for financial support and Dr. Dmytro Nykypanchuk and Dr. Jan Ilavsky for the help with USAXS analysis. The use of the Advanced Photon Source at Argonne National Laboratory was supported by the U.S. Department of Energy, Office of Science, Office of Basic Energy Sciences, under Contract DE-AC02-06CH11357.

References and Notes

(1) Bates, F. S.; Fredrickson, G. H. *Phys. Today* **1999**, *52* (2), 32–38.
(2) Park, C.; Yoon, J.; Thomas, E. L. *Polymer* **2003**, *44* (22), 6725–6760.
(3) O'Reilly, R. K.; Hawker, C. J.; Wooley, K. L. *Chem. Soc. Rev.* **2006**, *35* (11), 1068–1083.
(4) Jeong, B.; Bae, Y. H.; Lee, D. S.; Kim, S. W. *Nature (London)* **1997**, *388* (6645), 860–862.
(5) Stoykovich, M. P.; Muller, M.; Kim, S. O.; Solak, H. H.; Edwards, E. W.; de Pablo, J. J.; Nealey, P. F. *Science* **2005**, *308* (5727), 1442–1446.
(6) Matsen, M. W.; Bates, F. S. *Macromolecules* **1996**, *29* (4), 1091–1098.
(7) Bates, F. S.; Fredrickson, G. H. *Annu. Rev. Phys. Chem.* **1990**, *41*, 525–557.
(8) Deng, T.; Chen, C. T.; Honeker, C.; Thomas, E. L. *Polymer* **2003**, *44* (21), 6549–6553.
(9) Edrington, A. C.; Urbas, A. M.; DeRege, P.; Chen, C. X.; Swager, T. M.; Hadjichristidis, N.; Xenidou, M.; Fetters, L. J.; Joannopoulos, J. D.; Fink, Y.; Thomas, E. L. *Adv. Mater.* **2001**, *13* (6), 421–425.
(10) Urbas, A.; Sharp, R.; Fink, Y.; Thomas, E. L.; Xenidou, M.; Fetters, L. J. *Adv. Mater.* **2000**, *12* (11), 812–814.
(11) Hokajo, T.; Terao, K.; Nakamura, Y.; Norisuye, T. *Polym. J.* **2001**, *33* (6), 481–485.
(12) Lecommandoux, S.; Checot, F.; Borsali, R.; Schappacher, M.; Deffieux, A.; Brulet, A.; Cotton, J. P. *Macromolecules* **2002**, *35* (23), 8878–8881.
(13) Nakamura, Y.; Norisuye, T. *Polym. J.* **2001**, *33* (11), 874–878.
(14) Wintermantel, M.; Gerle, M.; Fischer, K.; Schmidt, M.; Wataoka, I.; Urakawa, H.; Kajiwara, K.; Tsukahara, Y. *Macromolecules* **1996**, *29* (3), 978–983.
(15) Bailly, C.; Stephenne, V.; Muchtar, Z.; Schappacher, M.; Deffieux, A. *J. Rheol.* **2003**, *47* (4), 821–827.
(16) Desvergne, S.; Heroguez, V.; Gnanou, Y.; Borsali, R. *Macromolecules* **2005**, *38* (6), 2400–2409.
(17) Inoue, T.; Matsuno, K.; Watanabe, H.; Nakamura, Y. *Macromolecules* **2006**, *39* (22), 7601–7606.
(18) Tsukahara, Y.; Namba, S.; Iwasa, J.; Nakano, Y.; Kaeriyama, K.; Takahashi, M. *Macromolecules* **2001**, *34* (8), 2624–2629.
(19) Vlassopoulos, D.; Fytas, G.; Loppinet, B.; Isel, F.; Lutz, P.; Benoit, H. *Macromolecules* **2000**, *33* (16), 5960–5969.
(20) Tsukahara, Y.; Miyata, M.; Senoo, K.; Yoshimoto, N.; Kaeriyama, K. *Polym. Adv. Technol.* **2000**, *11* (5), 210–218.
(21) Tsukahara, Y.; Ohta, Y.; Senoo, K. *Polymer* **1995**, *36* (17), 3413–3416.
(22) Wintermantel, M.; Fischer, K.; Gerle, M.; Ries, R.; Schmidt, M.; Kajiwara, K.; Urakawa, H.; Wataoka, I. *Angew. Chem., Int. Ed. Engl.* **1995**, *34* (13−14), 1472–1474.
(23) Rathgeber, S.; Pakula, T.; Wilk, A.; Matyjaszewski, K.; Lee, H. I.; Beers, K. L. *Polymer* **2006**, *47* (20), 7318–7327.
(24) Zhang, B.; Zhang, S. J.; Okrasa, L.; Pakula, T.; Stephan, T.; Schmidt, M. *Polymer* **2004**, *45* (12), 4009–4015.
(25) Bolisetty, S.; Airaud, C.; Xu, Y.; Muller, A. H. E.; Harnau, L.; Rosenfeldt, S.; Lindner, P.; Ballauff, M. *Phys. Rev. E* **2007**, *75*, 040803.
(26) Runge, M. B.; Dutta, S.; Bowden, N. B. *Macromolecules* **2006**, *39* (2), 498–508.
(27) Runge, M. B.; Bowden, N. B. *J. Am. Chem. Soc.* **2007**, *129* (34), 10551–10560.
(28) Ito, K.; Kawaguchi, S. Poly(macromonomers): Homo- and Copolymerization. In *Branched Polymers I*; Springer-Verlag: Berlin, 1999; Vol. 142, pp 129−178.
(29) Pyun, J.; Kowalewski, T.; Matyjaszewski, K. *Macromol. Rapid Commun.* **2003**, *24* (18), 1043–1059.
(30) Lee, H. I.; Matyjaszewski, K.; Yu-Su, S.; Sheiko, S. S. *Macromolecules* **2008**, *41* (16), 6073–6080.
(31) Mori, H.; Hirao, A.; Nakahama, S.; Senshu, K. *Macromolecules* **1994**, *27* (15), 4093–4100.
(32) Venkatesh, R.; Yajjou, L.; Koning, C. E.; Klumperman, B. *Macromol. Chem. Phys.* **2004**, *205* (16), 2161–2168.
(33) Benaglia, M.; Rizzardo, E.; Alberti, A.; Guerra, M. *Macromolecules* **2005**, *38* (8), 3129–3140.
(34) Ilavsky, J.; Allen, A. J.; Long, G. G.; Jemian, P. R. *Rev. Sci. Instrum.* **2002**, *73* (3), 1660–1662.
(35) Moad, G.; Rizzardo, E.; Thang, S. H. *Aust. J. Chem.* **2005**, *58* (6), 379–410.
(36) Beers, K. L.; Gaynor, S. G.; Matyjaszewski, K.; Sheiko, S. S.; Moller, M. *Macromolecules* **1998**, *31* (26), 9413–9415.
(37) Lee, H. I.; Jakubowski, W.; Matyjaszewski, K.; Yu, S.; Sheiko, S. S. *Macromolecules* **2006**, *39* (15), 4983–4989.
(38) Lohmeijer, B. G. G.; Pratt, R. C.; Leibfarth, F.; Logan, J. W.; Long, D. A.; Dove, A. P.; Nederberg, F.; Choi, J.; Wade, C.; Waymouth, R. M.; Hedrick, J. L. *Macromolecules* **2006**, *39* (25), 8574–8583.
(39) Gerle, M.; Fischer, K.; Roos, S.; Muller, A. H. E.; Schmidt, M.; Sheiko, S. S.; Prokhorova, S.; Moller, M. *Macromolecules* **1999**, *32* (8), 2629–2637.
(40) Fetters, L. J.; Lohse, D. J.; Milner, S. T.; Graessley, W. W. *Macromolecules* **1999**, *32* (20), 6847–6851.
(41) Dorgan, J. R.; Janzen, J.; Clayton, M. P.; Hait, S. B.; Knauss, D. M. *J. Rheol.* **2005**, *49* (3), 607–619.
(42) Roe, R. J. *Methods of X-Ray and Neutron Scattering in Polymer Science*; Oxford University Press: New York, 2000; p 196.
(43) Rathgeber, S.; Pakula, T.; Wilk, A.; Matyjaszewski, K.; Beers, K. L. *J. Chem. Phys.* **2005**, *122* (12), 13.

MA802304Y